Environmental Science and Pollution Research (2023) 30:93155–93164
https://doi.org/10.1007/s11356-023-28941-8

RESEARCH ARTICLE

Production of diesel-range oil through pyrolysis of polyolefins recovered from municipal solid waste

Ruming Pan[1] · Flávio Lopes Francisco Bittencourt[2,3] · Marcio Ferreira Martins[2] · Gérald Debenest[4]

Received: 25 August 2022 / Accepted: 19 July 2023 / Published online: 28 July 2023

Abstract

Pyrolysis is an effective method to valorize plastic waste and obtain value-added fuels. This study adopted the ANN-GA (artificial neural network-genetic algorithm) coupled with a central composition factorial design to optimize the oil production from the pyrolysis of waste polyolefins (WP). The interactive effects of PE mass fraction (20–80 wt%), residence time (20–60 min), and carrier gas flow rate (0–100 mL/min) on the yields of WP pyrolysis products were investigated extensively by ANN. Moreover, the highest WP pyrolysis oil production of 78.87 wt%, optimized by GA, was obtained under 80 wt% PE, 60 min, and 0 mL/min. It was found that the different conditions of PE mass fraction, residence time, and carrier gas flow rate did not change the types of oil's main functional groups ($-CH_2-$, $-C=C-$, $-C=CH_2$, $-CH_3$, and $=C-H$). The conditions affected the WP pyrolysis oil fractions significantly. The highest diesel selectivity of 91.42% was obtained under 20 wt% PE, 20 min, and 0 mL/min. Additionally, according to the interactive effects of different conditions on the productions of WP pyrolysis products, the pyrolysis pathways were proposed to understand the pyrolysis mechanism of WP better.

Keywords Waste polyolefins · Thermal decomposition · Diesel-range oil production · Artificial neural network · Genetic algorithm · Pyrolysis mechanism

Introduction

Municipal solid waste (MSW) accumulates promptly due to the huge consumption of resources and the low efficiency in recycling worldwide. Polyolefins of polyethylene (PE) and polypropylene (PP) are the most manufactured types of plastics, which accounted for 29.8% and 19.4% of total plastics produced, respectively (PlasticsEurope 2020). Moreover, waste polyolefins (WP) accounted for a large proportion of plastic waste in MSW (Aboulkas and El Bouadili 2010; Wang et al. 2020; Weckhuysen 2020). Also, the gravimetric composition of WP varies in different regions due to different local consumer demands. Therefore, it is highly imperative to find a resolution to valorize plastic waste, especially WP with different gravimetric compositions, into energy properly.

Pyrolysis or thermal decomposition is a useful way to convert WP into value-added fuels (Dobó et al. 2019; Fox and Stacey 2019; Zhang et al. 2020; Pan et al. 2021a), such as oil (gasoline and diesel) and gas (ethane and propane) (Butler et al. 2011; Benavides et al. 2017). Therefore, many studies have been explored extensively in order to better understand the pyrolysis of WP. One way to investigate the effects of operating parameters on pyrolysis is conducting thermogravimetric (TG) analysis. Although this analytical experiment is kinetically governed, some pyrolysis characteristics can be inferred. For instance, PE and PP's thermal decompositions took place within the temperature ranges of 355–477 °C and 329–467 °C, respectively (Li et al. 2016).

Marcio Ferreira Martins and Gérald Debenest contributed equally to this work.

Responsible Editor: Ta Yeong Wu

✉ Gérald Debenest
gerald.debenest@toulouse-inp.fr

[1] School of Energy Science and Engineering, Harbin Institute of Technology, Harbin 150001, China

[2] Laboratory of Combustion and Combustible Matter (LCC), PPGEM, Federal University of Espírito Santo, Vitória 29075-910, Brazil

[3] Federal Institute of Espirito Santo, 660 Augusto Costa de Oliveira St., Piuma 29285-000, Brazil

[4] Institut de Mécanique des Fluides de Toulouse (IMFT), Université de Toulouse, CNRS-INPT-UPS, 31400 Toulouse, France

Considering the gravimetric composition, 55 wt% of PE in WP changes the pyrolysis temperature range to 329–477 °C. In general, the literature reports that the decompositions of PE and PP were mainly processed from 400 to 500 °C (Jung et al. 2010), with the maximum pyrolysis rates at 462 °C and 451 °C, respectively (Ciliz et al. 2004; Duque et al. 2020). All these previous works were conducted with a low pyrolysis heating rate. Note that the maximum pyrolysis temperature of waste PE/PP is around 450 °C under TG conditions (Seo et al. 2003; Heydariaraghi et al. 2016; Miandad et al. 2016; Miandad et al. 2017; Santos et al. 2018; Milato et al. 2020; Ren and Huang, 2020; Jin et al. 2021).

The pyrolysis conversion is also sensible to other parameters than temperature and heating rate, such as gravimetric composition, carrier gas flow rate, and residence time. Although plenty of studies are devoted to solely determining the gravimetric composition's effect on pyrolysis oil production, other studies show that the parameters' interactions are dominated in oil production (Quesada et al. 2019). Nevertheless, most studies were conducted by adopting the one-factor-at-a-time statistical design (Papuga et al. 2016; Lopez et al. 2017; Kassargy et al. 2018; Santos et al. 2018; Parku et al. 2020). This method cannot capture the effects of variable interactions and may lead to misleading conclusions (Montgomery 2017). Therefore, we must implement a statistical method to reveal the parameters' interactions. Here, we present the use of an artificial neural network to correlate operating parameters and a genetic algorithm to optimize the process to obtain the highest oil yield.

WP gravimetric composition has a complicated impact on the oil production (Abnisa et al. 2019). Plenty of research efforts are devoted to determining the effect of WP gravimetric composition on the oil production. However, the intricate relationship between WP gravimetric composition and oil production is lacking till now. Therefore, this work performs twenty-one experiments, based on the central composition factorial design, to explore the interactive effects of the WP gravimetric composition, carrier gas flow rate, and residence time on oil yield and diesel selectivity (C9–C23). Based on the outcomes of the experiments, a hybrid model of a genetic algorithm coupled to an artificial neural network is used to optimize the oil production's conditions. Moreover, FTIR and GC/MS were used to qualify the oil's functional groups and components.

Materials and methods

Plastic samples

The samples of waste polyolefin (Fig. A.1) were purchased from Zhoushan Jinke Renewable Resources Co., Anhui, China. PE and PP were separately recovered from MSW and granulated into ~3 mm particles. The elemental analyses of PE and PP samples are listed in Table A.1.

Pyrolysis experiments

This work used the experimental setup developed in Pan et al. (2021b) and followed the same procedure to ensure an inert atmosphere by using the purge gas of nitrogen. The total mass of the gravimetric composition PE:PP used in each experiment was 5 g (± 0.001 g). The pyrolysis experiments were conducted at a moderate temperature of 450 °C and a low heating rate of 6 °C/min. The detailed conditions of the twenty-one pyrolysis experiments can be consulted in Table A.2, where gravimetric composition, carrier gas flow rate, and residence time were studied in the ranges of 20–80 wt%, 20–60 min, and 0–100 mL/min, respectively. Notably, 0 mL/min (non-sweeping atmosphere) indicates the nitrogen supply is stopped when the reactor starts to heat up. Following the central composition factorial design, fifteen experiments (T1–T15) were carried out to obtain the pyrolysis product yields for training the artificial neural network algorithm. Moreover, six other experiments (V1–V6) were carried out to acquire the experimental data for testing the artificial neural network algorithm. Each experiment was performed twice to ensure reproducibility.

Artificial neural network coupled with genetic algorithm

Figure A.2 sketches the methodology of coupling the genetic algorithm and artificial neural network. The artificial neural network was adopted to quantify the interactive effects of three independent variables (gravimetric composition, carrier gas flow rate, and residence time). The artificial neural network could be divided into three layers, i.e., input, hidden, and output (Rezk et al. 2022). Data training in the hidden layers established the mathematical expressions between the dependent and independent variables. Subsequently, the genetic algorithm optimized the relationship established by the artificial neural network (Pan et al. 2021a).

Oil characterization techniques

FTIR and GC/MS analyses were used to characterize oil products. Table A.3 summarizes the specific descriptions of both techniques.

Results and discussion

Accuracy of artificial neural network

Figure 1 depicts the experimental oil yields of the 21 experiments and the artificial neural network predictions in the

testing and training sets. The gas and char yields established by the artificial neural network are presented to verify the mass balance and idealize a pyrolysis pathway. Char yield is the percentage of final solid product in the total product. This study investigated the PE/PP co-pyrolysis under PE mass fraction of 20–80 wt%, residence time of 20–60 min, and carrier gas flow rate of 0–100 mL/min. The oil, gas (Fig. A.3a–b), and char (Fig. A.3c–d) yields hovered within the ranges of 64.24–78.87 wt%, 9.90–21.38 wt%, and 6.04–14.90 wt%, respectively. The yield of WP pyrolysis oil obtained by Quesada et al. (2020) was in the range of 56.90–68.10 wt%. Ahmad et al. (2015a) recovered 69.82 wt% and 80.88 wt% oil fractions, and 28.84 wt% and 17.24 wt% gas fractions from PP and PE thermal decompositions, respectively. Singh et al. (2019) conducted PE and PP pyrolysis at 450 °C. Consequently, gas yields of 8.5 wt% and 9.5 wt%, and char yields of 4 wt% and 8 wt% were obtained from PE and PP thermal decompositions, respectively. Mlynková et al. (2008) also carried out the pyrolysis of WP (75 wt% PE) at 450 °C. They recovered 79.7 wt% of oil, 14.4 wt% of gas, and 5.9 wt% of char, comparable to this study's values.

Compared with the artificial neural network predictions, the relative errors for oil yields — the target product of this work — were 1.1% in training and 2.6% in testing sets, while

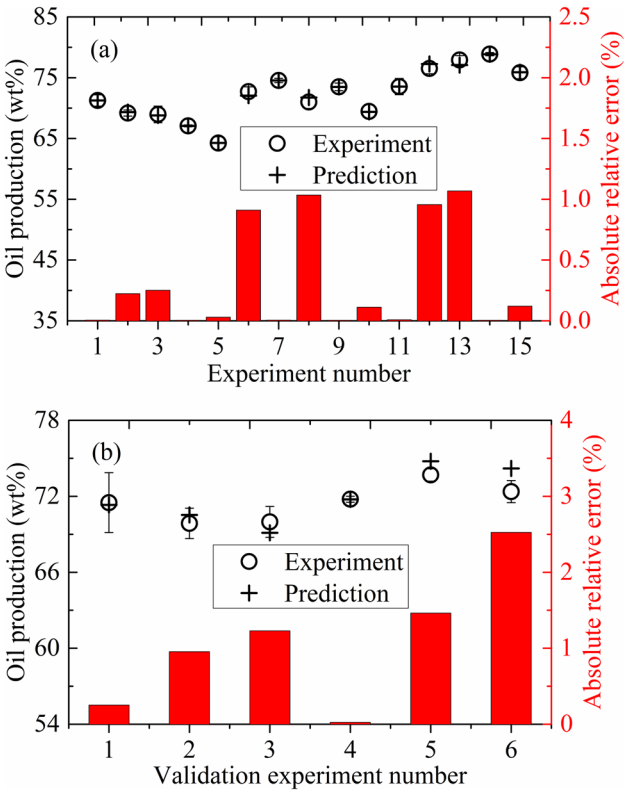

Fig. 1 Experimental and artificial neural network predicted productions of pyrolysis products in **a** training set and **b** testing set

the predicted gas and char yields had the maximum absolute relative errors of 6.07% and 2.65%, and 9.68% and 12.37% in the training and testing sets, respectively. Nonetheless, the global R-squared values and the average absolute relative deviations (AARD) between the experiments and the artificial neural network predictions were 0.9999 and 1.03%, and 0.9985 and 5.65% in training and testing sets, respectively. It indicated that the artificial neural network predictions were very accurate.

Interactive effects of conditions on oil yield

Figures 2 and A.4–6 depict the interactive effects of conditions on oil, gas, and char yields, respectively. The oil production raised from 64.20 to 79.00 wt% as the PE mass fraction increased (Figs. 2a and A.4a–b). The increase in oil production could be ascribed to the PE pyrolysis oil yield being higher than the PP pyrolysis oil yield under the same operating conditions in the case of being wholly decomposed at a moderate temperature (450–500 °C) (Kassargy et al. 2018; Singh et al. 2019; Quesada et al. 2020; Antelava et al. 2021). Figure A.5a–c show that the gas production decreased with the increasing PE mass fraction under longer residence times because the pyrolysis of PP could generate more gas products than PE pyrolysis (Quesada et al. 2020).

Longer residence time aggravated the WP pyrolysis oil's secondary cracking (Mastral et al. 2002; Hasan et al. 2021; Maqsood et al. 2021), thereby resulting in a reduction in the oil production (Figs. 2b and A.4c–d) and an enhancement in gas production (Fig. A.5d–e) under the PE mass fractions of 20 wt% and 50 wt%, respectively. Prolonged residence time might also convert oil into char through charring reactions (Williams and Slaney, 2007). Therefore, the char production increased with the increasing residence time (under 20 wt%, Fig. A.6d). The residence time had complex impacts on the oil (Fig. A.4d) and gas (Fig. A.5f) productions under 80 wt% PE. In the investigated residence time range, the oil production enhanced from 73.54 to 78.87 wt% under 0 mL/min and decreased from 77.25 to 75.91 wt% under 100 mL/min. Oppositely, the gas production reduced from 12.39 to 11.25 wt% under 0 mL/min and raised from 15.77 to 17.87 wt% under 100 mL/min. Extending the residence time would affect the oil and gas production in two ways: (i) exacerbating the oil's secondary cracking for oil depletion and gas generation (Pan et al. 2022), and (ii) promoting the gas recondensation for oil formation and gas consumption (Wang et al. 2019). The gas recondensation reaction dominated under lower carrier gas flow rates, which increased oil production and decreased gas production as the residence time prolonged. However, the oil secondary cracking reaction held a dominant position under higher flow rates of carrier gas, which were responsible for the reduction in oil production and the enhancement in gas production when the

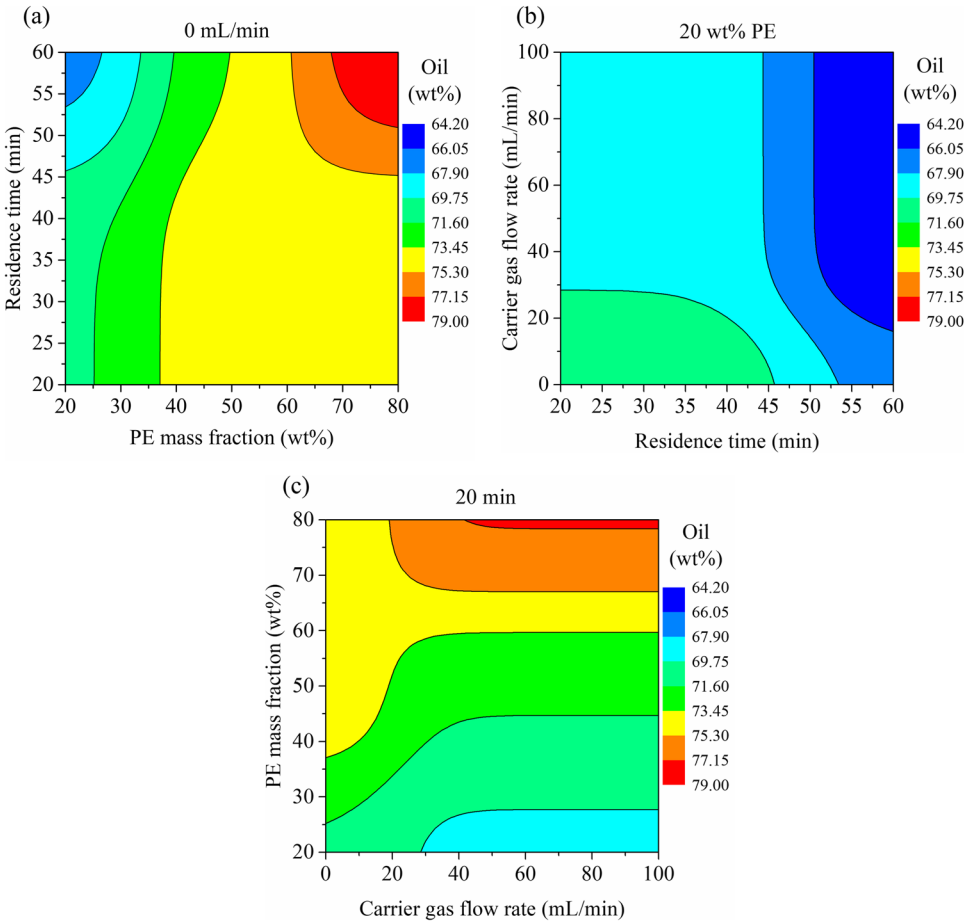

Fig. 2 Interactive effects of different conditions on oil yield under **a** 0 mL/min, **b** 20 wt% PE, and **c** 20 min, respectively

residence time extended. Char production was regulated by two reactions: (i) the char gasification reaction for char consumption and (ii) the oil charring reaction for char formation (Pan et al. 2021b). The char gasification reaction dominated the char production, thereby increasing the residence time resulted in a reduction in char production (6.46–6.07 wt%, Fig. A.6f).

The flow rate of carrier gas determines the duration of volatiles in the main reaction zone (Xu et al. 2020). Therefore, raising the flow rate of carrier gas could determine the oil production through three aspects: (i) shortening the duration of oil in the main reaction zone to suppress the oil secondary cracking for oil consumption (Pan and Debenest 2022), (ii) shortening the duration of gas in the main reaction zone to suppress the gas polycondensation and repolymerization for oil generation, and (iii) suppressing the oil charring for oil consumption (Pan et al. 2021b). Figures 2c and A.4e–f show that the oil production reduced with the raising carrier gas flow rate under shorter residence times (20–40 min) and lower PE mass fractions (20–68 wt%), indicating the suppressing of gas polycondensation and repolymerization dominated the oil production. However, the enhancement in carrier gas flow rate resulted in a rise in oil production under shorter residence times (20–40 min) and higher PE mass fractions (68–80 wt%), indicating the suppressing of oil secondary cracking and charring dominated the oil production. Figure A.4f shows that the oil production reduced with the improving carrier gas flow rate under the longest residence time (60 min), despite of the PE mass fraction's variation, which revealed that the oil production was dominated by the suppressing of gas polycondensation and repolymerization. On the other hand, the increase in carrier gas flow rate resulted in an enhancement in gas production (Fig. A.5g–i) due to the mass conservation of volatiles. Increasing the flow rate of carrier gas resulted in a decrease of 0.8 wt% in char production (Fig. A.6g–i), which could be contributed to the suppressing of oil charring reaction (Cheng et al. 2021).

Optimization of oil production by genetic algorithm

As discussed in the "Interactive effects of conditions on oil yield" section, it can be concluded that the gravimetric composition (PE mass fraction) and operating conditions (carrier gas flow rate and residence time) had a

complicated interaction on the oil production. Therefore, a genetic algorithm coupled to an artificial neural network was adopted to optimize oil production. Figure 3 exhibits that the highest oil production of 78.87 wt% was obtained under the PE mass fraction of 80 wt%, the residence time of 60 min, and the carrier gas flow rate of 0 mL/min. Table A.4 indicates that the optimized oil production obtained in this work is comparable to other studies. It should be noted that the volatiles could spontaneously flow out of the reactor at 0 mL/min because of the differential pressure arising from the WP pyrolysis process (Muhammad et al. 2019; Singh et al. 2019).

FTIR analysis

Figure 4 shows that the FTIR spectral peaks' abscissas (wavelength) were the same in different oil samples, indicating that the main functional groups' types were not affected by the gravimetric composition and operating conditions (Pan et al. 2021b). Table A.5 lists the specific main functional groups of the oil sample under the optimal condition (80 wt% PE, 60 min, and 0 mL/min), which are $-CH_2-$, $-C=C-$, $-C=CH_2$, $-CH_3$, and $=C-H$. The WP pyrolysis oil samples were mainly composed of alkanes and alkenes (Ahmad et al. 2015b; Alves et al. 2021).

GC-MS analysis

Figure 5 depicts the carbon number's distributions of the oil samples under different conditions. The oil from the thermal cracking of WP was composed of hydrocarbons ranging from C8 to C34 (Costa et al. 2021; Gu et al. 2020; Zhou et al. 2021). Hydrocarbons of C9, C10, C13, C15, and C17 accounted for the most significant proportions in the oil. Figures 5a and A.7 show that the

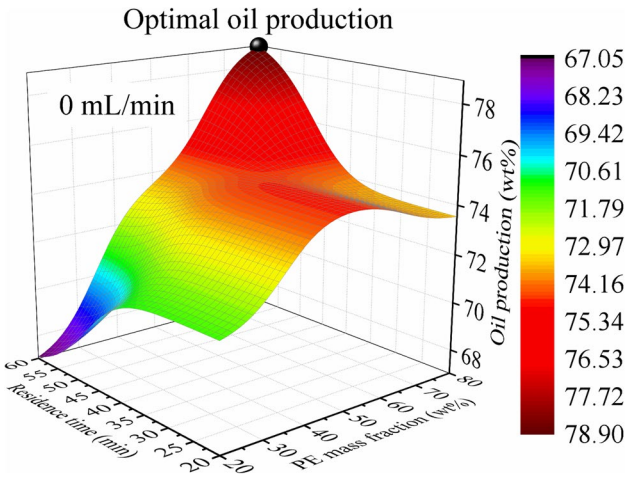

Fig. 3 Optimization of oil production by genetic algorithm

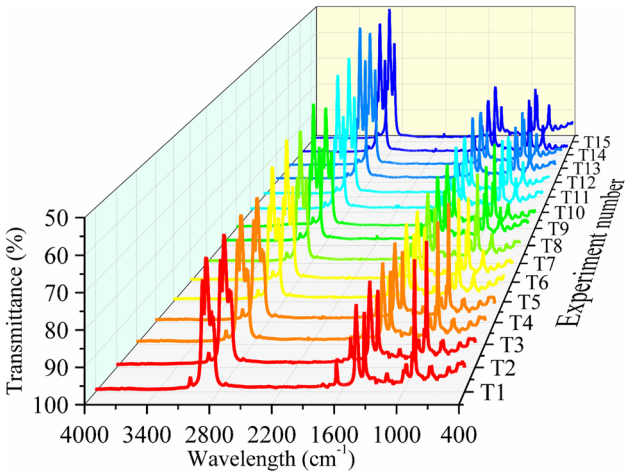

Fig. 4 FTIR spectra of oil samples

carbon number distributions were similar under the same gravimetric composition, regardless of the changes in operating conditions. The increase in PE mass fraction in WP resulted in a dramatic reduction in C9, C10, and

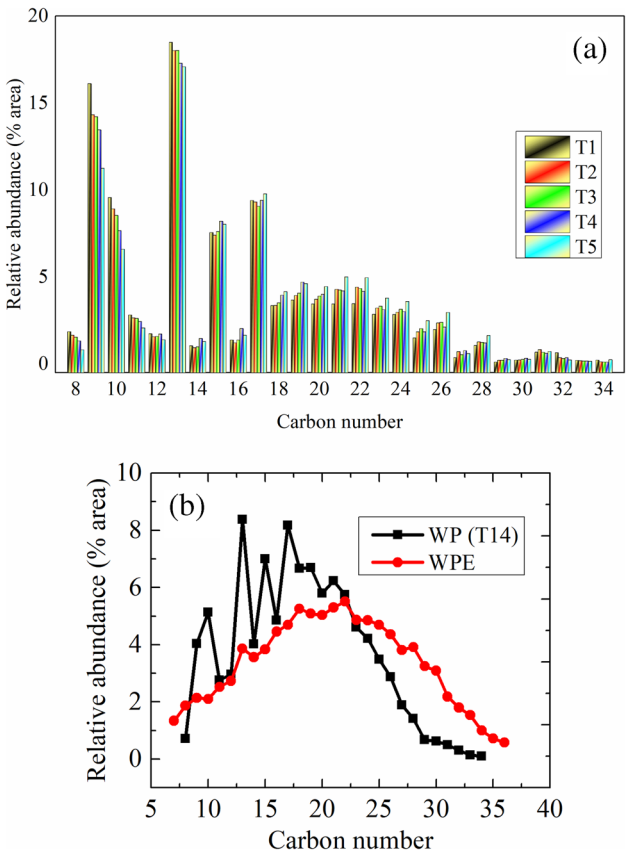

Fig. 5 Carbon number distributions of the oil samples under different conditions: **a** T1–5 under 20 wt% PE; **b** WP and WPE pyrolysis oils (Pan et al. 2021b)

C13. When the PE mass fraction enhanced from 20 wt% (T4) to 80 wt% (T14), C9, C10, and C13 proportions reduced from 13.46 to 4.03%, from 7.66 to 5.13%, and from 17.92 to 8.38%, respectively. This could be ascribed to the reduction of PP content, which can generate large proportions of C9, C10, and C13 (Zhou et al. 2021; Rezk et al. 2022). It is worth noting that when hydrocarbons exceeded C21, the enhancement in the carbon number resulted in a reduction in the proportion of hydrocarbons. Taking sample T14 into consideration, the proportion of hydrocarbons reduced from 6.23 to 0.10% as the carbon number increased from C21 to C34.

Figure 5b illustrates the difference in carbon number distribution between WP (sample T14) and waste PE (WPE) (Pan et al. 2021b) pyrolysis oil samples. The WP pyrolysis oil had higher contents of hydrocarbons ranging from C9 to C21. On the other hand, hydrocarbons ranging from C23 to C36 accounted for more enormous proportions in the WPE pyrolysis oil, attributing to the long carbon chain structure in WPE (Miandad et al. 2017).

The oil can be classified into different fractions based on the carbon number (Yang et al. 2016; Luo et al. 2020). In this study, the oil was categorized as light (C8–C12), middle (C13–C20), and heavy (C21–C34) fractions (Costa et al. 2021; Zhou et al. 2021). Figure A.8 shows that the middle fraction occupied the most significant proportion in oil. The light, middle, and heavy fractions hovered within the ranges of 13.87–32.09%, 42.81–52.85%, and 19.58–43.12%, respectively. Consequently, the mean molecular weight of WP pyrolysis oil fluctuated within a relatively wide range of 215.62–270.79 g/mol. The light, middle, and heavy fractions were 32.56%, 44.99%, and 23.30% in sole PE pyrolysis oil; and 15.16%, 51.81%, and 33.02% in sole PP pyrolysis oil, respectively (Ahmad et al. 2015a). These results were within the ranges of WP pyrolysis oil fractions obtained in this study.

Figure 6 depicts the effects of operating conditions and gravimetric composition on the distributions of mean molecular weight and oil fractions. Figure 6a demonstrates that the raise in PE mass fraction led to a reduction in the light fraction and an enhancement in the heavy fraction, whereas it had little effect on the middle fraction. Consequently, the oil's mean molecular weight raised from 224.45 to 252.65 g/mol as the PE mass fractions increased, which could be ascribed to the PE pyrolysis oil being heavier than the PP pyrolysis oil (Zhou et al. 2021). The WP pyrolysis oil was much lighter than the PE pyrolysis oil, of which the mean molecular weight hovered within the range of 291.00–325.23 g/mol (Pan et al. 2021b).

Figure 6b shows that prolonging residence time would decrease the light fraction and increase the heavy fraction, whereas it slightly impacted the middle fraction. Accordingly, the extension of residence time resulted in a persistently increase (from 239.90 to 256.44 g/mol) in the mean molecular weight of WP pyrolysis oil, which was contributed to the intensified secondary cracking of oil's light fraction (López et al. 2011; Wang et al. 2021).

Figure 6c illustrates that the increase in carrier gas flow rate resulted in a reduction in both light and middle fractions and an increase in the heavy fraction. Improved flow rate

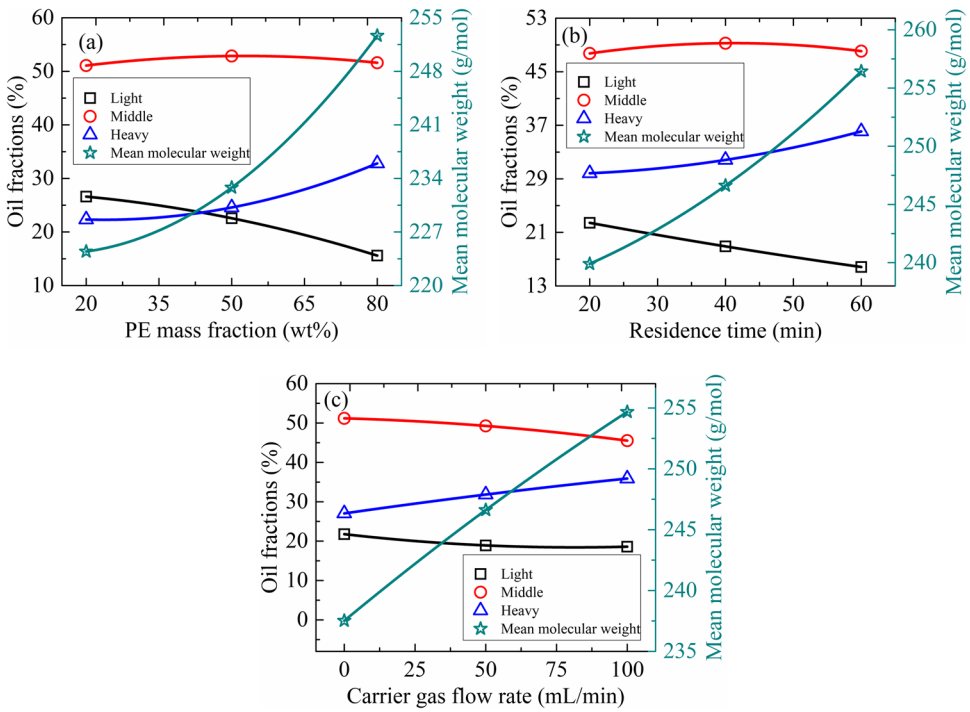

Fig. 6 Effects of gravimetric composition and operating conditions on the distributions of oil fractions and mean molecular weight: **a** PE mass fraction (samples of T4, T9, and T14); **b** residence time (samples of T6, V4, and T10); **c** carrier gas flow rate (samples of T7, V4, and T8)

of carrier gas shortened the duration of pyrolytic volatiles in the main reaction zone, which regulated the oil fractions in four ways: (i) inhibiting the heavy fraction's secondary cracking for the formation of middle and light fractions, and for the consumption of heavy fraction, (ii) inhibiting the middle fraction's secondary cracking for the light fraction formation and the middle fraction consumption, (iii) inhibiting the light fraction's secondary cracking for the light fraction consumption, and (iv) suppressing the gas polycondensation for the light fraction formation (Xu et al. 2020; Pan et al. 2021b). The experimental results revealed that (i) and (iv) dominated the formation of oil fractions when the carrier gas flow rate changed. Therefore, the mean molecular weight of pyrolytic oil increased from 237.52 to 254.68 g/mol as the carrier gas flow rate raised.

Diesel selectivity

The WP pyrolytic oil could be served as a proxy for commercial diesel (ranging from C9 to C24 (Milato et al. 2020)). Therefore, the interactions of operating conditions and gravimetric composition on the oil's diesel selectivity had been evaluated through the artificial neural network. Figure A.9 shows that the pyrolytic oil's diesel selectivity varied from 79.02 to 91.18%. Moreover, Fig. 7 shows that the highest diesel selectivity of 91.42% was obtained under the PE mass fraction of 20 wt%, the residence time of 20 min, and the carrier gas flow rate of 0 mL/min (non-sweeping atmosphere).

Reaction pathways

Figure 8 shows that the random and chain-end scissions predominated in the initial stage of WP pyrolysis. WP was decomposed into a small amount of volatiles (gas and oil)

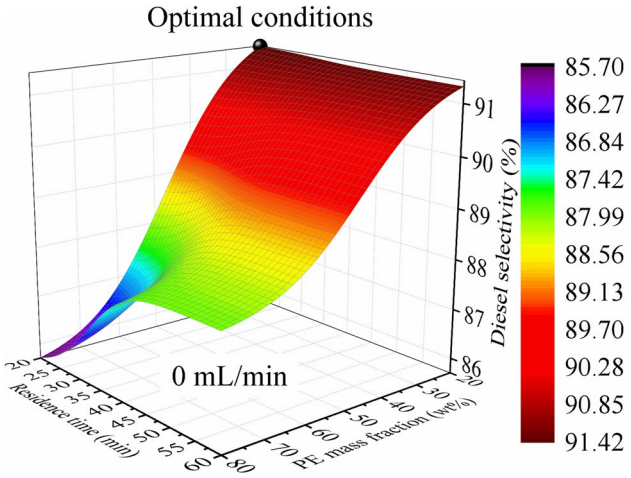

Fig. 7 Optimization of diesel selectivity by genetic algorithm

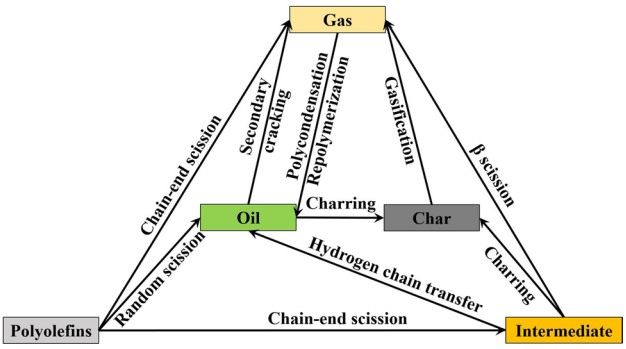

Fig. 8 Schematic diagram of pyrolysis mechanism of WP

and a large amount of intermediate product (wax) (Wong and Broadbelt 2001; Onwudili et al. 2009). The oil produced was mainly composed of low-molecular alkenes (Das and Tiwari 2018). The experimental results showed that the increase in residence time led to a decrease in light fraction and an increase in heavy fraction. This is because that the proportion of low-molecular alkenes generated in the initial stage was decreased under longer residence times. In the mid-stage of WP thermal decomposition, the intermediate was further pyrolyzed into oil (alkanes and alkenes) through hydrogen transfer reactions to a great extent. As shown in Fig. A.11, the formations of alkanes and alkenes were attributed to intermolecular and intramolecular hydrogen transfer reactions (Zolghadr et al. 2021; Rodríguez-Luna et al. 2021), respectively. Part of char and gas were simultaneously generated through the intermediate's charring and β scission reactions. Subsequently, part of the oil's light fraction was ulteriorly decomposed into gas and char through the secondary cracking and charring reactions in the late stage of WP pyrolysis, respectively. Therefore, the experimental oil production decreased, gas production increased, and char production increased with the increasing residence time. In the meantime, part of the gas (olefins) was synthesized into light-fraction oil through the polycondensation and repolymerization reactions. A small part of char was also pyrolyzed into gas through the gasification reactions in this stage.

Conclusion

This study quantitatively investigated the interactions of operating conditions and gravimetric composition on the oil production from the WP pyrolysis. The ANN-GA coupled with a central composition factorial design was utilized to obtain the highest oil yield. The findings revealed that the highest oil yield of 78.87 wt% was obtained under 80 wt% PE, 60 min, and 0 mL/min. The increases in PE mass fraction, residence time, and carrier gas flow rate resulted in a decrease in light fraction and an increase in heavy fraction,

thereby leading to the production of heavier oil with a larger mean molecular weight. The oil's diesel selectivity was used as a quality index of WP pyrolysis oil. The highest diesel selectivity of 91.42% was obtained under 20 wt% PE, 20 min, and 0 mL/min. Moreover, the WP optimal pyrolysis conditions for specific regions could be obtained via ANN-GA coupled with a central composition factorial design.

Supplementary Information The online version contains supplementary material available at https://doi.org/10.1007/s11356-023-28941-8.

Acknowledgements Thanks are given to Dr. Yue ZAN from LCC-CNRS-UPS for her assistance in the FTIR test and analysis.

Author contribution All authors contributed to the study conception and design. Material preparation, data collection, and analysis were performed by RP, FLFB, MFM, and GD. The first draft of the manuscript was written by RP and all authors commented on previous versions of the manuscript. All authors read and approved the final manuscript.

Data availability The datasets used and/or analyzed during the current study are available from Ruming Pan on reasonable request.

Declarations

Ethics approval and consent to participate Not applicable.

Consent for publication Not applicable.

Competing interests The authors declare no competing interests.

References

Abnisa F, Anuar Sharuddin SD, bin Zanil MF, WMA WD, Indra Mahlia TM (2019) The yield prediction of synthetic fuel production from pyrolysis of plastic waste by Levenberg–Marquardt approach in feedforward neural networks model. Polymers 11(11):1853. https://doi.org/10.3390/polym11111853

Aboulkas A, El Bouadili A (2010) Thermal degradation behaviors of polyethylene and polypropylene. Part I: pyrolysis kinetics and mechanisms. Energy Conv Manag 51(7):1363–1369. https://doi.org/10.1016/j.enconman.2009.12.017

Ahmad I, Khan MI, Khan H, Ishaq M, Tariq R, Gul K, Ahmad W (2015a) Influence of metal-oxide-supported bentonites on the pyrolysis behavior of polypropylene and high-density polyethylene. J Appl Polym Sci 132:41221. https://doi.org/10.1002/app.41221

Ahmad I, Khan MI, Khan H, Ishaq M, Tariq R, Gul K, Ahmad W (2015b) Pyrolysis study of polypropylene and polyethylene into premium oil products. Int J Green Energy 12(7):663–671. https://doi.org/10.1080/15435075.2014.880146

Alves O, Nobre C, Durão L, Monteiro E, Brito P, Gonçalves M (2021) Effects of dry and hydrothermal carbonisation on the properties of solid recovered fuels from construction and municipal solid wastes. Energy Conv Manag 237:114101. https://doi.org/10.1016/j.enconman.2021.114101

Antelava A, Jablonska N, Constantinou A, Manos G, Salaudeen SA, Dutta A, Al-Salem SM (2021) Energy potential of plastic waste valorization: a short comparative assessment of pyrolysis versus gasification. Energ Fuel 35(5):3558–3571. https://doi.org/10.1021/acs.energyfuels.0c04017

Benavides PT, Sun P, Han J, Dunn JB, Wang M (2017) Life-cycle analysis of fuels from post-use non-recycled plastics. Fuel 203:11–22. https://doi.org/10.1016/j.fuel.2017.04.070

Butler E, Devlin G, McDonnell K (2011) Waste polyolefins to liquid fuels via pyrolysis: review of commercial state-of-the-art and recent laboratory research. Waste Biomass Valori 2(3):227–255. https://doi.org/10.1007/s12649-011-9067-5

Cheng F, Tompsett GA, Alvarez DVF, Romo CI, McKenna AM, Niles SF, Nelson RK, Reddy CM, Granados-Fócil S, Paulsen AD, Zhang R (2021) Metal oxide supported Ni-impregnated bifunctional catalysts for controlling char formation and maximizing energy recovery during catalytic hydrothermal liquefaction of food waste. Sustain Energy Fuels 5(4):941–955. https://doi.org/10.1039/D0SE01662D

Ciliz NK, Ekinci E, Snape CE (2004) Pyrolysis of virgin and waste polypropylene and its mixtures with waste polyethylene and polystyrene. Waste Manage 24(2):173–181. https://doi.org/10.1016/j.wasman.2003.06.002

Costa CS, Muñoz M, Ribeiro MR, Silva JM (2021) A thermogravimetric study of HDPE conversion under a reductive atmosphere. Catalysis Today 379:192–204. https://doi.org/10.1016/j.cattod.2020.07.021

Das P, Tiwari P (2018) The effect of slow pyrolysis on the conversion of packaging waste plastics (PE and PP) into fuel. Waste Manage 79:615–624. https://doi.org/10.1016/j.wasman.2018.08.021

Dobó Z, Jakab Z, Nagy G, Koós T, Szemmelveisz K, Muránszky G (2019) Transportation fuel from plastic wastes: production, purification and SI engine tests. Energy 189:116353. https://doi.org/10.1016/j.energy.2019.116353

Duque JVF, Martins MF, Debenest G, Orlando MTDA (2020) The influence of the recycling stress history on LDPE waste pyrolysis. Polym Test 86:106460. https://doi.org/10.1016/j.polymertesting.2020.106460

Fox JA, Stacey NT (2019) Process targeting: an energy based comparison of waste plastic processing technologies. Energy 170:273–283. https://doi.org/10.1016/j.energy.2018.12.160

Gu J, Fan H, Wang Y, Zhang Y, Yuan H, Chen Y (2020) Co-pyrolysis of xylan and high-density polyethylene: product distribution and synergistic effects. Fuel 267:116896. https://doi.org/10.1016/j.fuel.2019.116896

Hasan MM, Rasul MG, Khan MMK, Ashwath N, Jahirul MI (2021) Energy recovery from municipal solid waste using pyrolysis technology: a review on current status and developments. Renewable Sustainable Energy Rev 145:111073. https://doi.org/10.1016/j.rser.2021.111073

Heydariaraghi M, Ghorbanian S, Hallajisani A, Salehpour A (2016) Fuel properties of the oils produced from the pyrolysis of commonly-used polymers: effect of fractionating column. J Anal Appl Pyrolysis 121:307–317. https://doi.org/10.1016/j.jaap.2016.08.010

Jin K, Vozka P, Gentilcore C, Kilaz G, Wang NHL (2021) Low-pressure hydrothermal processing of mixed polyolefin wastes into clean fuels. Fuel 294:120505. https://doi.org/10.1016/j.fuel.2021.120505

Jung SH, Cho MH, Kang BS, Kim JS (2010) Pyrolysis of a fraction of waste polypropylene and polyethylene for the recovery of BTX aromatics using a fluidized bed reactor. Fuel Process Technol 91(3):277–284. https://doi.org/10.1016/j.fuproc.2009.10.009

Kassargy C, Awad S, Burnens G, Kahine K, Tazerout M (2018) Gasoline and diesel-like fuel production by continuous catalytic pyrolysis of waste polyethylene and polypropylene mixtures over USY zeolite. Fuel 224:764–773. https://doi.org/10.1016/j.fuel.2018.03.113

Li K, Lee SW, Yuan G, Lei J, Lin S, Weerachanchai P, Yang Y, Wang JY (2016) Investigation into the catalytic activity of microporous

and mesoporous catalysts in the pyrolysis of waste polyethylene and polypropylene mixture. Energies 9(6):431. https://doi.org/10.3390/en9060431

López A, De Marco I, Caballero BM, Laresgoiti MF, Adrados A (2011) Influence of time and temperature on pyrolysis of plastic wastes in a semi-batch reactor. Chem Eng J 173(1):62–71. https://doi.org/10.1016/j.cej.2011.07.037

Lopez G, Artetxe M, Amutio M, Bilbao J, Olazar M (2017) Thermochemical routes for the valorization of waste polyolefinic plastics to produce fuels and chemicals. A review. Renewable Sustainable Energy Rev 73:346–368. https://doi.org/10.1016/j.rser.2017.01.142

Luo W, Hu Q, Fan ZY, Wan J, Luo B, Yan ZX, Huang SX, Zhou Z (2020) Co-pyrolysis characteristics of different reworked synthetic polymer types. J Energy Inst 93(6):2232–2237. https://doi.org/10.1016/j.joei.2020.06.005

Maqsood T, Dai J, Zhang Y, Guang M, Li B (2021) Pyrolysis of plastic species: a review of resources and products. J Anal Appl Pyrolysis 159:105295. https://doi.org/10.1016/j.jaap.2021.105295

Mastral FJ, Esperanza E, Garcıa P, Juste M (2002) Pyrolysis of high-density polyethylene in a fluidised bed reactor. Influence of the temperature and residence time. J Anal Appl Pyrolysis 63(1):1–15. https://doi.org/10.1016/S0165-2370(01)00137-1

Miandad R, Barakat MA, Aburiazaiza AS, Rehan M, Ismail IMI, Nizami AS (2017) Effect of plastic waste types on pyrolysis liquid oil. Int Biodeterior Biodegrad 119:239–252. https://doi.org/10.1016/j.ibiod.2016.09.017

Miandad R, Nizami AS, Rehan M, Barakat MA, Khan MI, Mustafa A, Ismail IMI, Murphy JD (2016) Influence of temperature and reaction time on the conversion of polystyrene waste to pyrolysis liquid oil. Waste Manage 58:250–259. https://doi.org/10.1016/j.wasman.2016.09.023

Milato JV, França RJ, Rocha AS, Calderari MRM (2020) Catalytic co-pyrolysis of oil sludge with HDPE to obtain paraffinic products over HUSY zeolites prepared by dealumination and desilication. J Anal Appl Pyrolysis 151:104928. https://doi.org/10.1016/j.jaap.2020.104928

Mlynková B, Hájeková E, Bajus M (2008) Copyrolysis of oils/waxes of individual and mixed polyalkenes cracking products with petroleum fraction. Fuel Process Technol 89(11):1047–1055. https://doi.org/10.1016/j.fuproc.2008.04.007

Montgomery DC (2017) Design and analysis of experiments. John Wiley & Sons

Muhammad I, Makwashi N, Manos G (2019) Catalytic degradation of linear low-density polyethylene over HY-zeolite via pre-degradation method. J Anal Appl Pyrolysis 138:10–21. https://doi.org/10.1016/j.jaap.2018.11.025

Onwudili JA, Insura N, Williams PT (2009) Composition of products from the pyrolysis of polyethylene and polystyrene in a closed batch reactor: effects of temperature and residence time. J Anal Appl Pyrolysis 86(2):293–303. https://doi.org/10.1016/j.jaap.2009.07.008

Pan R, Debenest G (2022) Numerical investigation of a novel smoldering-driven reactor for plastic waste pyrolysis. Energy Conv Manag 257:115439. https://doi.org/10.1016/j.enconman.2022.115439

Pan R, Duque JVF, Debenest G (2021a) Investigating waste plastic pyrolysis kinetic parameters by genetic algorithm coupled with thermogravimetric analysis. Waste Biomass Valori 12(5):2623–2637. https://doi.org/10.1007/s12649-020-01181-4

Pan R, Martins MF, Debenest G (2021b) Pyrolysis of waste polyethylene in a semi-batch reactor to produce liquid fuel: optimization of operating conditions. Energy Conv Manag 237:114114. https://doi.org/10.1016/j.enconman.2021.114114

Pan R, Martins MF, Debenest G (2022) Optimization of oil production through ex-situ catalytic pyrolysis of waste polyethylene with activated carbon. Energy 248:123514. https://doi.org/10.1016/j.energy.2022.123514

Papuga SV, Gvero PM, Vukić LM (2016) Temperature and time influence on the waste plastics pyrolysis in the fixed bed reactor. Therm Sci 20(2):731–741. https://doi.org/10.2298/TSCI141113154P

Parku GK, Collard FX, Görgens JF (2020) Pyrolysis of waste polypropylene plastics for energy recovery: influence of heating rate and vacuum conditions on composition of fuel product. Fuel Process Technol 209:106522. https://doi.org/10.1016/j.fuproc.2020.106522

PlasticsEurope (2020) An analysis of European plastics production, demand and waste data. Plastics – the Facts https://www.plasticseurope.org/en/resources/publications/4312-plastics-facts-2020

Quesada L, Calero M, Martín-Lara MA, Perez A, Blazquez G (2020) Production of an alternative fuel by pyrolysis of plastic wastes mixtures. Energ Fuel 34(2):1781–1790. https://doi.org/10.1021/acs.energyfuels.9b03350

Quesada L, Pérez A, Godoy V, Peula FJ, Calero M, Blázquez G (2019) Optimization of the pyrolysis process of a plastic waste to obtain a liquid fuel using different mathematical models. Energy Conv Manag 188:19–26. https://doi.org/10.1016/j.enconman.2019.03.054

Ren X, Huang Z (2020) Pyrolysis of milk bottle wastes of polypropylene and high density polyethylene: determination of kinetic and thermodynamic parameters. Energy Sources A: Recovery Util Environ Eff:1–18. https://doi.org/10.1080/15567036.2020.1804488

Rezk H, Mohammed RH, Rashad E, Nassef AM (2022) ANFIS-based accurate modeling of silica gel adsorption cooling cycle. Sustain Energy Technol Assess 50:101793. https://doi.org/10.1016/j.seta.2021.101793

Rodríguez-Luna L, Bustos-Martínez D, Valenzuela E (2021) Two-step pyrolysis for waste HDPE valorization. Process Saf Environ Prot 149:526–536. https://doi.org/10.1016/j.psep.2020.11.038

Santos BPS, Almeida D, Maria de Fatima VM, Henriques CA (2018) Petrochemical feedstock from pyrolysis of waste polyethylene and polypropylene using different catalysts. Fuel 215:515–521. https://doi.org/10.1016/j.fuel.2017.11.104

Seo YH, Lee KH, Shin DH (2003) Investigation of catalytic degradation of high-density polyethylene by hydrocarbon group type analysis. J Anal Appl Pyrolysis 70(2):383–398. https://doi.org/10.1016/S0165-2370(02)00186-9

Singh RK, Ruj B, Sadhukhan AK, Gupta P (2019) Thermal degradation of waste plastics under non-sweeping atmosphere: part 1: effect of temperature, product optimization, and degradation mechanism. J Environ Manage 239:395–406. https://doi.org/10.1016/j.jenvman.2019.03.067

Wang C, Lei H, Qian M, Huo E, Zhao Y, Zhang Q, Mateo W, Lin X, Kong X, Zou R, Ruan R (2020) Application of highly stable biochar catalysts for efficient pyrolysis of plastics: a readily accessible potential solution to a global waste crisis. Sustain Energy Fuels 4(9):4614–4624. https://doi.org/10.1039/D0SE00652A

Wang F, Gao N, Quan C (2021) Effect of hot char and steam on products in waste tire pressurized pyrolysis process. Energy Conv Manag 237:114105. https://doi.org/10.1016/j.enconman.2021.114105

Wang Z, Liu K, Xie L, Zhu H, Ji S, Shu X (2019) Effects of residence time on characteristics of biochars prepared via co-pyrolysis of sewage sludge and cotton stalks. J Anal Appl Pyrolysis 142:104659. https://doi.org/10.1016/j.jaap.2019.104659

Weckhuysen BM (2020) Creating value from plastic waste. Science 370(6515):400–401. https://doi.org/10.1126/science.abe3873

Williams PT, Slaney E (2007) Analysis of products from the pyrolysis and liquefaction of single plastics and waste plastic mixtures. Resour Conserv Recycl 51(4):754–769. https://doi.org/10.1016/j.resconrec.2006.12.002

Wong HW, Broadbelt LJ (2001) Tertiary resource recovery from waste polymers via pyrolysis: neat and binary mixture reactions of polypropylene and polystyrene. Ind Eng Chem 40(22):4716–4723. https://doi.org/10.1021/ie010171s

Xu F, Ming X, Jia R, Zhao M, Wang B, Qiao Y, Tian Y (2020) Effects of operating parameters on products yield and volatiles

composition during fast pyrolysis of food waste in the presence of hydrogen. Fuel Process Technol 210:106558. https://doi.org/10.1016/j.fuproc.2020.106558

Yang J, Rizkiana J, Widayatno WB, Karnjanakom S, Kaewpanha M, Hao X, Abudula A, Guan G (2016) Fast co-pyrolysis of low density polyethylene and biomass residue for oil production. Energy Conv Manag 120:422–429. https://doi.org/10.1016/j.enconman.2016.05.008

Zhang D, Lin X, Zhang Q, Ren X, Yu W, Cai H (2020) Catalytic pyrolysis of wood-plastic composite waste over activated carbon catalyst for aromatics production: effect of preparation process of activated carbon. Energy 212:118983. https://doi.org/10.1016/j.energy.2020.118983

Zhou N, Dai L, Lv Y, Li H, Deng W, Guo F, Chen P, Lei H, Ruan R (2021) Catalytic pyrolysis of plastic wastes in a continuous microwave assisted pyrolysis system for fuel production. Chem Eng J 418:129412. https://doi.org/10.1016/j.cej.2021.129412

Zolghadr A, Sidhu N, Mastalski I, Facas G, Maduskar S, Uppili S, Go T, Neurock M, Dauenhauer PJ (2021) On the method of pulse-heated analysis of solid reactions (PHASR) for polyolefin pyrolysis. ChemSusChem 14(19):4214–4227. https://doi.org/10.1002/cssc.202002667